International Journal of Precision Engineering and Manufacturing (2023) 24:547–553
https://doi.org/10.1007/s12541-022-00746-8

Online ISSN 2005-4602
Print ISSN 2234-7593

REGULAR PAPER

Morphologies of Cemented Tungsten Carbides Irradiated by Femtosecond Laser with High Pulse Energy for Machining Enhanced Cutting Tools

Young-Gwan Shin[1,2] · **Junha Choi**[1,2] · **Sung-Hak Cho**[1,2]

Received: 14 September 2022 / Revised: 28 October 2022 / Accepted: 8 November 2022 / Published online: 21 February 2023

Abstract
Recently, ultrafast laser machining has been used to machine hard materials. Ultrafast laser machining can be precisely machined without a non-thermal effect or damage to machining tools. However, their morphologies differed depending on the pulse energy. Generally, to machine difficult-to-machine materials, hard materials are irradiated by laser pulses with high pulse energy. Laser pulses with high pulse energy remove large volumes. However, burrs are formed at the top surface, and the large volumes removed remain empty. These burrs and empty spaces reduce the efficiency of the process. Owing to these problems, the formation of burrs must be restricted during laser ablation. Accordingly, this work aimed to reduce the formation of burrs and improve the machining efficiency. In this study, to overcome the aforementioned undesirable effects, the position of a focused laser beam with a high pulse energy was altered when irradiating cemented tungsten carbides; the laser had a pulse duration of 190 fs, wavelength of 1026 nm, frequency of 6 kHz, and pulse energy of 100 μJ. When focused laser beam was irradiated at the ablated bottom surface, the laser machining efficiency increased. Moreover, the position of the focused laser beam affected the morphology of burrs. On focusing the laser beam at the surface, burrs with shorter heights and larger lengths were formed. The morphologies of these burrs and the ablated space affected the laser passing rate and machining efficiency.

Keywords Ultrafast laser · Focused laser beam position · Cemented carbide · Morphological characteristics

1 Introduction

Laser machining is a technology widely employed in various industries and has many advantages as a non-contact method. Undesired effects such as machining tool wear, fracture, and replacement costs incurred by contact methods are avoided with non-contact machining [1, 2]. In addition, ultrafast laser can be used for precise machining on difficult-to-cut materials with high precision and flexibility by tightly focusing a laser beam [3, 4].

Among difficult-to-cut materials, cemented tungsten carbides have superior mechanical hardness and wear resistance and are employed in aerospace, machining tools, and press-stamping because of their ability to maintain their original stiffness at high temperatures [5, 6]. Generally, cemented tungsten carbides are machined using electrical discharge machining (EDM) or grinding. However, EDM and grinding induce the wear or even failure of cutting tools composed of cemented tungsten carbides. These approaches also result in the formation of heat effected zones (HAZs) [7]. Recently, cemented tungsten carbides have been investigated for laser machining applications to overcome the problems [8–10].

Laser machining is affected by various parameters, including laser wavelength, pulse duration, and pulse type etc. Among the laser parameters, the pulse duration of the laser can classify the laser as a nanosecond, picosecond, or femtosecond laser. Heat accumulation during laser ablation is a major property [11–13]. When a nanosecond laser irradiates the surface of a material, the laser energy is absorbed by the surface of the material, where melt pool formation and

✉ Sung-Hak Cho
shcho@kimm.re.kr

[1] Department of Nano-Manufacturing Technology, Korea Institute of Machinery & Materials (KIMM), 156, Gajeongbuk-Ro, Yuseong-Gu, Daejeon, South Korea

[2] Department of Nano-Mechatronics, University of Science and Technology (UST), 217, Gajeong-Ro, Yuseong-Gu, Daejeon, South Korea

vaporization occur owing to the absorbed laser beam. The vapor-induced recoil pressure pushes the melted material outside the pool. In addition, the Marangoni effect occurs because of the temperature gradient of the melt pool. Therefore, the melted materials flow from the hot center to the cold edge [14]. The melted and flowing materials become burrs and particles. Furthermore, cracks occur inside the material due to heat effects. Post-processing is required to remove burrs and cracks. Post-processing increases manufacturing costs and time.

The heat effect is a major cause of burr formation. Therefore, to decrease the burrs, an ultrafast laser with a short pulse duration can be employed. A shorter pulse duration results in a smaller heat effect. Recently, machining using ultrafast lasers has been investigated [15, 16]. When the ultrafast laser was irradiated at the workpiece surface, the irradiated material evaporates before transferring heat to an adjacent area [17]. Thus, the heat effect can be decreased, and various materials can be quickly and precisely ablated [18].

Nevertheless, burrs have been observed in studies that employed ultrafast lasers with various materials [10, 19–21]. Wu et al. focused on the burrs in stainless steel, where a 10 ps laser with a wavelength of 532 nm and pulse energy of 3 μJ was used [10]. Further, Bian et al. reported the formation of burrs in indium tin-oxide when using a 60 fs laser with a wavelength of 800 nm and pulse energy of 125–310 nJ [19]. Zhao et al. conducted hole drilling on Ti alloy, Cu, Al alloy, and Ni alloy, by using a 10 ps laser with a wavelength of 532 nm and a maximum pulse energy of 135 μJ [20]. Wang et al. also studied holes drilling on ceramics, with the use of lasers with various pulse durations [21]. These previous studies indicate that burrs are formed regardless of the laser parameters, and that lasers with femtosecond pulse durations and a high pulse energy are insufficient. However, thus far, analyses of the formation burrs have not been reported. To improve the quality of ultrafast laser machining, further research on burr formation is imperative. However, research on the formation of burrs using femtosecond lasers is insufficient. In the study, we studied the interaction between cemented tungsten carbides and a femtosecond laser with high pulse energy to realize the many ablated volume. In addition, the position of the laser-focused beam was regulated to change the properties of the laser beam.

Understanding the interaction between femtosecond lasers and the burr formation of cemented tungsten carbides is important for the widespread application of laser machining in various industries. To understand the interaction between the laser parameters and cemented tungsten carbides, we analyzed the diameter, depth, and morphology of the machined hole. These results will be useful for laser machining technology without the formation of burrs.

2 Experimental Setup

We performed machining by changing the position of the pulsed laser-focused beam. We irradiated laser pulses with 1026 nm of center wavelength, 190 fs. The laser beam diameters were 30, 47, and 52 μm at the positions of focus, defocus_4 μm, and defocus_8 μm, respectively. A vibrator was used to change the position of the laser-focused beam and couple it to the objective lens. In this study, we used a 50× objective lens with a 0.42 NA and 1.60 μm DOF (Depth of Field) (Mitutoyo, Japan) to focus the laser beam. The objective lens was equipped with a vibrator (P-726; Physik Instrumente, Karlsruhe, Germany) to change the position of the focused laser beam. A function generator (NF Corporation, Yokohama, Japan) was used to change the position of the pulsed laser-focused beam. The input voltage to the vibrator was controlled using a function generator and monitored using an oscilloscope (Tektronix, Beaverton, OR, USA). Consequently, the position of the focused laser beam can be regulated. Figure 1 shows the proposed laser machining system.

We investigated two ablation methods by changing the position of the laser-focused beam. In the first method, the workpieces were irradiated with a pulsed laser with 50 laser counts. Once the pulsed laser focus beam was located on the workpiece surface, it was defocused to 4 and 8 μm below the surface. In the second method, we changed the pulsed laser focal beam position step-by-step using the following four schemes: First, type A was irradiated with 50 laser counts on the surface of the cemented tungsten carbide. Second, in type B, the initial 10 laser counts were irradiated on the surface and 40 laser counts were irradiated 4 μm below the initial position of the pulsed laser focus beam. Third, in type C, the initial 10 laser counts were irradiated on the surface and 40 laser counts were irradiated 8 μm below the initial

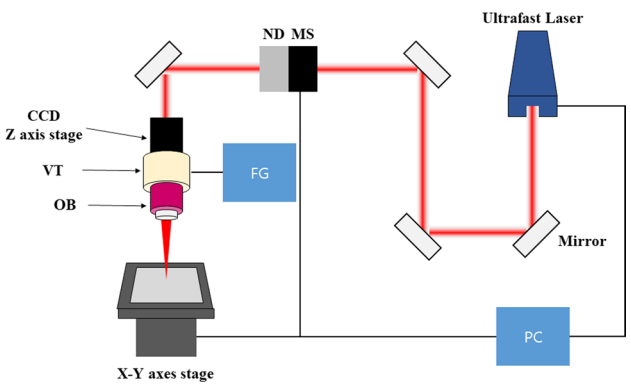

Fig. 1 Schematic of ultrafast laser machining system (*ND* Neutral-density filter; *MS* Mechanical shutter; *CCD* Charge-coupled device; *OB* Objective lens; *VT* vibrator; *FG* Function generator)

Table 1 Focused laser beam position changes for each machining type

Machining types	Number of laser pulses		
	~10 pulses	11–30 pulses	31–50 pulses
A	Focus_0 μm	Focus_0 μm	Focus_0 μm
B	Focus_0 μm	Defocus_4 μm	Defocus_4 μm
C	Focus_0 μm	Defocus_8 μm	Defocus_8 μm
D	Focus_0 μm	Defocus_4 μm	Defocus_8 μm

position of the pulsed laser focus beam. Finally, in type D, the initial 10 laser counts were irradiated on the surface, 20 laser counts were irradiated 4 μm below the initial position of the pulsed laser focus beam, and the final 20 laser counts were irradiated 4 μm below (total:8 μm) the prior 4-μm position of the pulsed laser focus beam. The machining types are listed in Table 1.

In this study, the thickness of the cemented tungsten carbide was 1 mm, and the material comprised 90% WC and 10% Co. The laser used was a Pharos SP manufactured by Light Conversion (Lithuania). The central wavelength of Pharos SP was 1026 nm, and the pulse width was 190 fs. In addition, the maximum pulse energy was 1 mJ at a repetition rate of 6 kHz, and M^2 was 1.3. Laser pulse energies of 100 μJ were used at a repetition rate of 6 kHz. The morphologies were analyzed using a scanning electron microscopy (SEM; SM-350, Topcon, Japan; S-4800, Hitachi, Japan) and confocal laser scanning microscopy (VK-1000, Keyence, Japan).

3 Results and Discussions

We analyzed the morphologies of the holes ablated by laser pulsed beams depending on the positions of the focused laser beam with 100 μJ of laser energy. The height and length of the burrs were measured. Once the length of the burrs was determined, as shown in Fig. 2a, we observed that the length of the burrs increased as the laser beam was defocused in Fig. 2b. The height of the burrs were determined using confocal laser scanning microscopy (VK-1000, Keyence, Japan), as shown in Fig. 3a. Figure 3b shows that as the laser beam was focused, a higher burr height was formed. The temperatures of electrons and lattices are important in femtosecond laser machining. To predict temperature changes, we used the two-temperature method (TTM), which describes the temperature evolution of electrons and lattice systems via two differential equations:

$$C_e \frac{\partial T_e}{\partial t} = \frac{\partial}{\partial z}\left(k_e \frac{\partial T_e}{\partial z}\right) - \gamma\left(T_e - T_i\right) + S \tag{1}$$

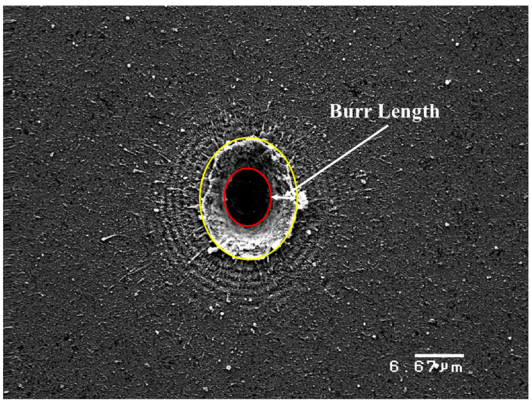

(a)

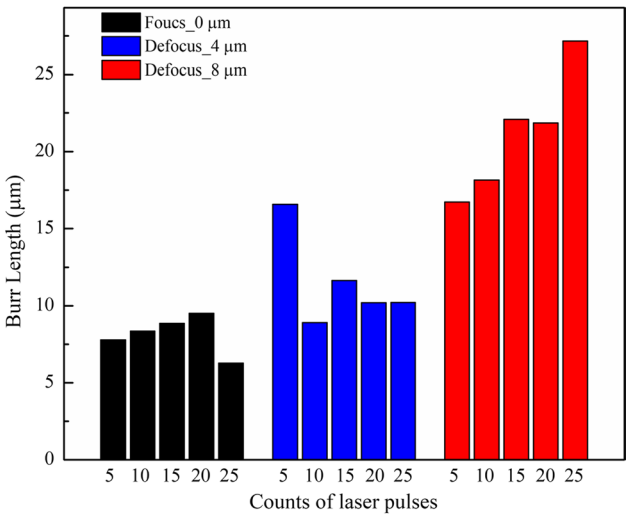

(b)

Fig. 2 Burr lengths irradiated by laser pulse with 100 μJ in various focus position and counts of laser pulses: **a** determining a burr length, **b** Burr lengths depending on focus position and counts of laser pulses

$$C_i \frac{\partial T_i}{\partial t} = \frac{\partial}{\partial z}\left(k_i \frac{\partial T_i}{\partial z}\right) + \gamma\left(T_e - T_i\right) \tag{2}$$

$$S = I(x,t) * (1-R) * \alpha * \exp(-\alpha * y) \tag{3}$$

$$\mathrm{I(x,t)} = \mathrm{I_0} * \exp\left(-\mathrm{x^2/r^2}\right) * \exp\left(-3.5(\mathrm{t}-\tau)^2/\tau^2\right) \tag{4}$$

where C is the heat capacity of the electrons and the lattice, as denoted by subscripts e and i, respectively. S, γ, k_e, k_i, α, R, and τ denote the laser source, electron–photon coupling coefficient, electron thermal conductivity, lattice thermal conductivity, absorption coefficient, reflectivity, and pulse duration, respectively (Table 2).

When the materials were irradiated by a pulsed laser beam with a femtosecond laser, the electrons were rapidly excited. The excited electrons collide with each other. The collided electron-induced energy is transferred to the lattice.

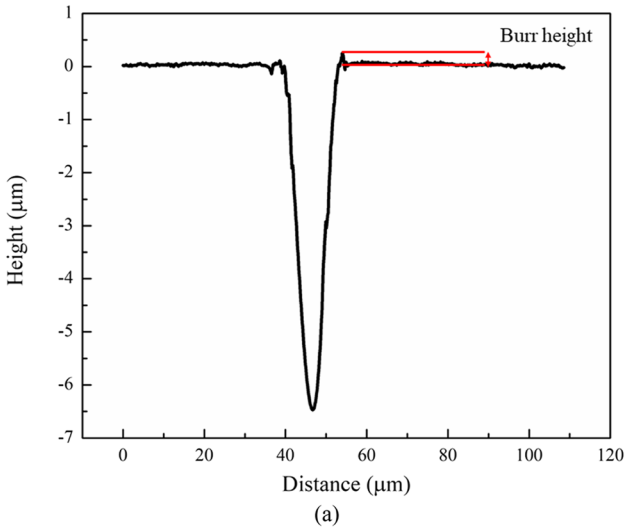

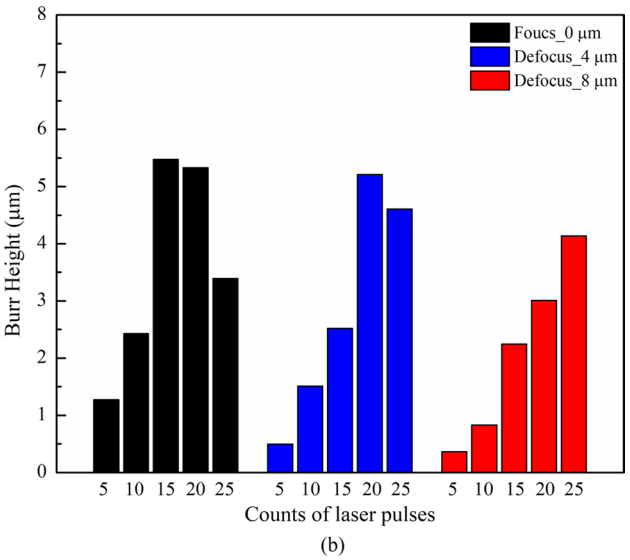

Fig. 3 Burr height irradiated by laser pulse with 100 μJ in various focus position and counts of laser pulses: **a** determining a burr height, **b** Burr height depending on focus position and counts of laser pulses

Table 2 Properties of the cemented tungsten carbides

k_e [W/(m*K)]	k_i [W/(m*K)]	α[cm^{-1}]	R	γ [$W/m^{-3}K^{-1}$]
84.02*(T_e/T_i)	144.5	2.5*10^{-5}	0.46	1.65*10^{17}

The heated lattice transfers heat to the surrounding area. The heat transfer was completed until the temperature of the electron equaled to the temperature of the lattice [7, 22]. Beam diameters were calculated using the D^2 method [23]. The D^2 method was mainly used to calculate the diameter of the laser beam through the interrelation of laser energy and diameter formed by laser pulses. The diameters of the laser-focused, defocused_4 μm, and defocused_8 μm beams are 30, 47, and 52 μm, respectively. The temperature changes of the electrons and lattice were calculated, as shown in Fig. 4. The many induced electrons are generated by excited electrons irradiated by the laser pulses [24]. Many electrons induce enhanced nonlinear effects, such as multi-phonon absorption and avalanche ionization [25]. Therefore, when the same surface of the cemented tungsten carbides was irradiated, the maximum temperature of the electrons differed depending on the focus of the laser beam. The highest temperature was achieved under irradiation by the focused laser beam. Furthermore, under the equilibrium state, the temperatures of the electrons and lattices were higher for the focused laser beam, as compared with those for the unfocused laser beam. This higher temperature of the electrons and the equilibrium of the electrons and lattices affected physical phenomena. Specifically, owing to the higher temperature, the cemented tungsten carbides underwent vaporization. When the focused laser beam was located at the ablated bottom surface, an additional amount of the cemented tungsten carbides was removed, as shown in Fig. 5, under irradiation by the multi-pulse laser. We also observed that the diameter of the holes varied depending on the type of machining. When the focused laser beam was positioned at the top surface, various physical phenomenon such as plasma and shockwaves led to additional ablation at the top surface of the cemented tungsten carbides. As a result, the 25 μm of diameter was acquired. Similarly, when the focused laser beam was positioned at the ablated bottom surface, various physical phenomena occurred in the interior of the cemented tungsten carbides. Accordingly, when the focused laser beam was positioned at the ablated bottom surface, the diameter of the holes decreased. The length of the burrs under machining type A was 7.9 μm, similar

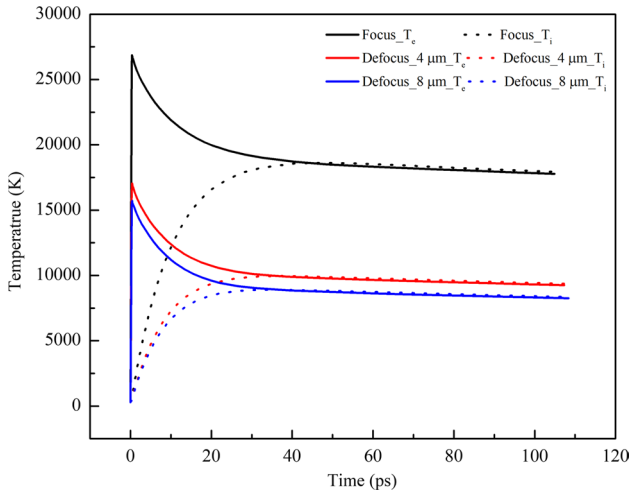

Fig. 4 Temperature and time to reach thermal equilibrium analyzed by TTM: the time to reach thermal equilibrium irradiated by 100 μJ depending a position of laser focused beam (T_e: the temperature of electron system, T_i: the temperature of lattice system)

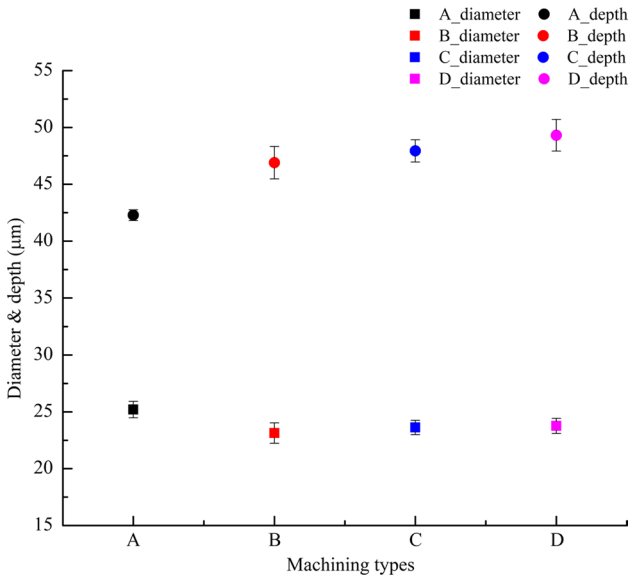

Fig. 5 Diameters and depths of ablated holes with different machining types and laser pulse energies of 100 μJ

to that under machining type B (7.9 μm) but shorter than those under machining types C and D (i.e., 9.5 and 10.2 μm, respectively). The height of the burrs under machining type A was 4.7 μm, similar to those under machining types B and D but shorter than that under machining type C (5.9 μm). When the focused laser beam was irradiated at the surface, a higher temperature distribution was formed. The majority of cemented tungsten carbides were removed by the rapid rise in temperature-induced vaporization. However, the edges of the focused laser beam had a lower temperature owing to the properties of the Gaussian laser beam. The area irradiated by the edges of the Gaussian laser beam remains melted. In addition, a higher temperature induced tensile stress inside cemented tungsten carbides [26, 27]. The tensile stress was pushed away from the center. Consequently, burrs with higher heights were formed (Fig. 6).

It was observed that the rapid temperature affected the morphologies of the burrs at the surface of the cemented tungsten carbides. Laser pulses were irradiated by changing the position of the laser-focused beam. The ablated bottom surface was irradiated with a laser-focused beam. The changes in the positions of the laser-focused beams are listed in Table 1. To change the position of the laser-focused beam, the diameters of the ablated holes were 25 μm. However, the depth of the ablated holes differed depending on the machining type. In addition, the change in the position of the laser-focused beam affects the lengths and heights of the burrs.

The initial 10 laser pulses were irradiated at the top surface regardless of the machining type. The focused laser beam was located at the ablated bottom surface after the initial 10 laser pulses. The location of focused laser beam was in the gap between the top and ablated bottom surfaces. The length of the burrs increased depending on the machining type. When the laser-focused beam was located at the ablated bottom surface, the top surface was irradiated at the edge area of the Gaussian laser beam. For a Gaussian laser beam, the edge area has lower laser energy. Lower laser energy induced a smaller temperature increase. For a lower temperature of electrons increase, the major material removal mechanism is the heat process. Consequently, the

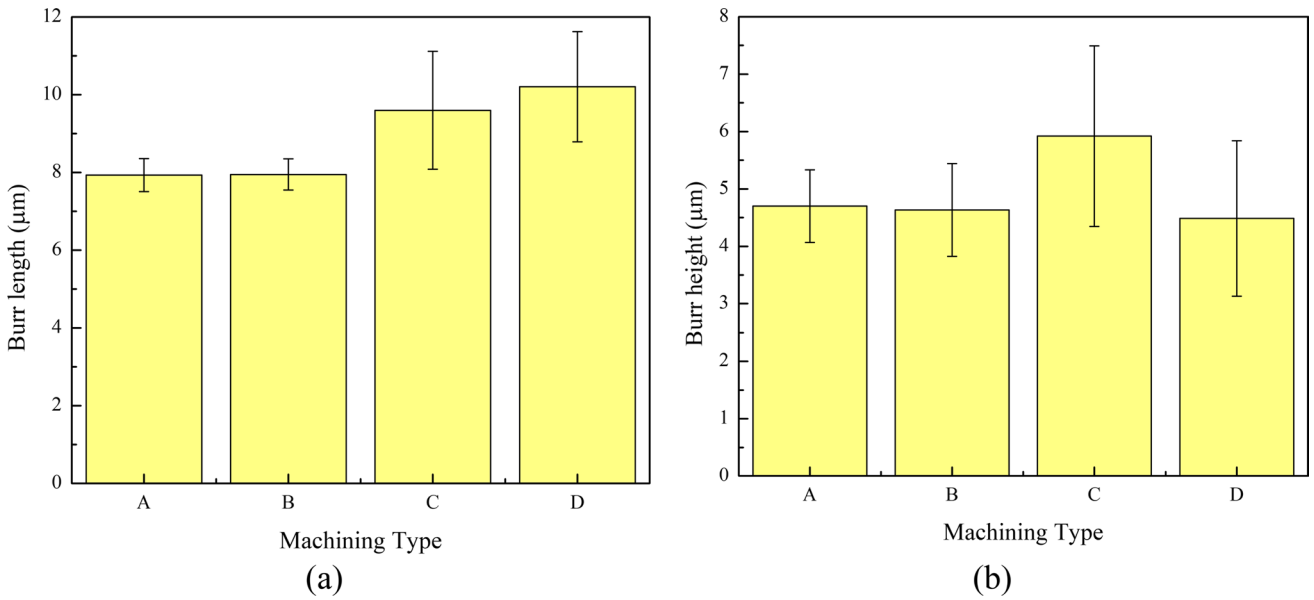

Fig. 6 Measured length and height of burrs depending on machining types: **a** a measured length of burrs, **b** a measured height of burrs

lengths of burrs were longer. For machining types B and C, the position of the laser-focused beam is changed once. For machining type D, the position was changed twice. The height of the burrs was shorter in machining type D than in machining types B and C. If the laser pulses with high energy were irradiated to the same spot, a large amount of material will be removed. In addition, the height of the burrs increased. However, enhanced depths of the holes were obtained in machining type D than in machining type A. Therefore, the heights of the burrs are similar. Under irradiation using laser pulses with a high pulse energy, burr formation is inevitable. However, burrs with shorter heights and larger lengths help improve the laser energy efficiency [10]. For laser machining with multi-pulse lasers, the laser energy efficiency can be expressed as in Eqs. (5) and (6):

$$N = 1-\exp\left(-2r_d^2/\,w\left(Z_F\right)^2\right) \tag{5}$$

$$I_{c(n+1)} = I_{ni} * N_n \tag{6}$$

where r_d is the radius of the burrs, $w(Z_F)$ is the beam size, N is the laser passing rate, and I is the laser intensity. Burrs with larger heights reduced the laser passing rate, leading to a decrease in the machining efficiency. Thus, positioning the focused laser beam at the ablated bottom surface is advantages for machining via multi-pulse lasers with a high pulse energy.

4 Conclusion

We investigated the interaction between cemented tungsten carbides and a femtosecond laser with high pulse energy. In addition, we analyzed the diameter, depth, and morphology of the holes. When the laser focused beam was irradiated at a surface, the maximum temperature of the electrons is high. At high electron temperatures, a mount of cemented tungsten carbides was removed. However, the laser-induced heat created a melted state of cemented tungsten. In addition, the high-temperature induced tensile stress was pushed away. Therefore, high heights were formed.

Under irradiation by a multi-pulse laser with a high laser pulse energy, burrs were formed. On focusing the laser beam, shorter burrs with larger heights were observed. By contrast, when the focused laser beam was incident on the ablated bottom surface, burrs with shorter heights and larger lengths were formed. The height and length of these burrs affected the laser efficiency; specifically, burrs with shorter heights and larger lengths increased the laser passing rate. Accordingly, machining type D was observed to improve the machining efficiency.

Recently, laser machining with high pulse energy and many laser pulses has been required because of the properties of the materials. Subsequently, the removal of many materials induces a laser-defocused beam and reduces the laser energy efficiency. Understanding the interaction between the high pulse energy of the femtosecond laser and cemented tungsten carbides is helpful for laser processes requiring high pulse energy.

References

1. Yang, L., Wei, J., Ma, Z., Song, P., Ma, J., Zhao, Y., Huang, Z., Zhang, M., Yang, F., & Wang, X. (2019). The fabrication of micro/nano structures by laser machining. *Nanomaterials, 9*, 1789. https://doi.org/10.3390/nano9121789
2. Nakajima, A., & Yan, J. (2022). Response of resin coating films containing fine metal particles to ultrashort laser pulses. *International Journal of Precision Engineering and Manufacturing, 23*, 385–393. https://doi.org/10.1007/s12541-022-00629-y
3. Dumitru, G., Romano, V., Weber, H. P., Sentis, M., & Marine, W. (2002). Femtosecond ablation of ultrahard materials. *Applied Physics A: Materials Science & Processing, 74*, 729–739. https://doi.org/10.1007/s003390101183
4. Gu, B. (2004). Ultrafast laser applications in semiconductor industry. *Proceedings of SPIE Photon Processing in Microelectronics and Photonics, III*(5339), 226. https://doi.org/10.1117/12.529794
5. Jia, K., Fischer, T. E., & Gallois, B. (1998). Microstructure, hardness and toughness of nanostructured and conventional WC-Co composites. *Nanostructured Materials, 10*, 875–891. https://doi.org/10.1016/S0965-9773(98)00123-8
6. Prakash, L. J. (1995). Application of fine grained tungsten carbide based cemented carbides. *International Journal of Refractory Metals and Hard Materials, 13*, 257–264. https://doi.org/10.1016/0263-4368(95)92672-7
7. Eberle, G., & Wegener, K. (2014). Ablation study of WC and PCD composites using 10 picosecond and 1 nanosecond pulse durations at green and infrared wavelengths. *Physics Procedia, 56*, 951–962. https://doi.org/10.1016/j.phpro.2014.08.115
8. Guimarães, B., Figueiredo, D., Fernandes, C. M., Silva, F. S., Miranda, G., & Carvalho, O. (2019). Laser machining of WC-Co green compacts for cutting tools manufacturing. *International Journal of Refractory Metals and Hard Materials, 81*, 316–324. https://doi.org/10.1016/j.ijrmhm.2019.03.018
9. Wang, X., & Zheng, H. (2018). Picosecond laser micro-drilling, engraving and surface texturing of tungsten carbide. *Journal of Laser Applications, 30*, 032203. https://doi.org/10.2351/1.5040602
10. Wu, H., Zou, P., Cao, J., & Ehmann, K. F. (2020). Vibrating-lens-assisted laser drilling. *Journal of Manufacturing Processes, 55*, 389–398. https://doi.org/10.1016/j.jmapro.2020.03.005
11. Chen, J., An, Q., Ming, W., & Chen, M. (2021). Investigations on continuous-wave laser and pulsed laser induced controllable ablation of SiCf/SiC composites. *Journal of the European Ceramic Society, 41*, 5835–5849. https://doi.org/10.1016/j.jeurceramsoc.2021.04.061
12. Link, S., Burda, C., Mohamed, M. B., Nikoobakht, B., & El-Sayed, M. A. (1999). Laser photothermal melting and fragmentation of gold nanorods: Energy and laser pulse-width dependence. *Journal of Physical Chemistry A, 103*, 1165–1170. https://doi.org/10.1021/jp983141k
13. Bityurin, N., & Malyshev, A. (2002). Bulk photothermal model for laser ablation of polymers by nanosecond and subpicosecond

pulses. *Journal of Applied Physics, 92*, 605–613. https://doi.org/10.1063/1.1486040
14. Pinkerton, A. J., & Li, L. (2004). Modelling the geometry of a moving laser melt pool and deposition track via energy and mass balances. *Journal of Physics D Applied Physics, 37*, 1885–1895. https://doi.org/10.1088/0022-3727/37/14/003
15. Malinauskas, M., Žukauskas, A., Hasegawa, S., Hayasaki, Y., Mizeikis, V., Buividas, R., & Juodkazis, S. (2016). Ultrafast laser processing of materials: From science to industry. *Light: Science and Applications, 5*, e16133. https://doi.org/10.1038/lsa.2016.133
16. Sugioka, K., & Cheng, Y. (2014). Ultrafast lasers—reliable tools for advanced materials processing. *Light: Science and Applications, 3*, e149. https://doi.org/10.1038/lsa.2014.30
17. Dausinger, F. (2001). Laser drilling with short pulses. *XIII International Symposium on Gas Flow and Chemical Lasers and High-power Laser Conference, 4184*, 519. https://doi.org/10.1117/12.413990
18. Kononenko, T. V., Garnov, S. V., Klimentov, S. M., Konov, V. I., Loubnin, E. N., Dausinger, F., Raiber, A., & Taut, C. (1997). Laser ablation of metals and ceramics in picosecond-nanosecond pulsewidth in the presence of different ambient atmospheres. *Applied Surface Science, 109–110*, 48–51. https://doi.org/10.1016/S0169-4332(96)00905-1
19. Bian, Q., Yu, X., Zhao, B., Chang, Z., & Lei, S. (2013). Femtosecond laser ablation of indium tin-oxide narrow grooves for thin film solar cells. *Optics & Laser Technology, 45*, 395–401. https://doi.org/10.1016/j.optlastec.2012.06.018
20. Zhao, W., Liu, H., Shen, X., Wang, L., & Mei, X. (2020). Percussion drilling hole in Cu, Al Ti and Ni alloys using ultra-short pulsed laser ablation. *Materials (Basel)*. https://doi.org/10.3390/ma13010031
21. Wang, H., Lin, H., Wang, C., Zheng, L., & Hu, X. (2017). Laser drilling of structural ceramics—a review. *Journal of the European Ceramic Society, 37*, 1157–1173. https://doi.org/10.1016/j.jeurceramsoc.2016.10.031
22. Perry, M. D., Stuart, B. C., Banks, P. S., Feit, M. D., Yanovsky, V., & Rubenchik, A. M. (1999). Ultrashort-pulse laser machining of dielectric materials. *Journal of Applied Physics, 85*, 6803–6810. https://doi.org/10.1063/1.370197
23. Liu, J. M. (1982). Simple technique for measurements of pulsed Gaussian-beam spot sizes. *Optics Letters, 7*, 196. https://doi.org/10.1364/ol.7.000196
24. Tani, G., Orazi, L., Fortunato, A., & Cuccolini, G. (2008). Laser ablation of metals: A 3D process simulation for industrial applications. *Journal of Manufacturing Science and Engineering, Transactions of the ASME, 130*, 0311111–03111111. https://doi.org/10.1115/1.2917326
25. Di Niso, F., Gaudiuso, C., Sibillano, T., Mezzapesa, F. P., Ancona, A., & Lugarà, P. M. (2014). Role of heat accumulation on the incubation effect in multi-shot laser ablation of stainless steel at high repetition rates. *Optics Express, 22*, 12200. https://doi.org/10.1364/oe.22.012200
26. Colombier, J. P., Combis, P., Stoian, R., & Audouard, E. (2007). High shock release in ultrafast laser irradiated metals: Scenario for material ejection. *Physical Review B: Condensed Matter and Materials Physics, 75*, 1–11. https://doi.org/10.1103/PhysRevB.75.104105
27. Kautek, W., Rudolph, P., Daminelli, G., & Krüger, J. (2005). Physico-chemical aspects of femtosecond-pulse-laser-induced surface nanostructures. *Applied Physics A: Materials Science & Processing, 81*, 65–70. https://doi.org/10.1007/s00339-005-3211-7

Young-Gwan Shin received an M. Sc. Degree in Nanomechatronics from the University of Science and Technology. His research interests are Femtosecond laser ablation and advanced laser microprocessing technology. He is currently a Ph. D. student at the University of Science and Technology.

Junha Choi received an M. Sc. Degree in Nanomechatronics from the University of Science and Technology. His research interests are Femtosecond laser ablation and advanced laser microprocessing technology. He is currently a Ph. D. student at the University of Science and Technology.

Sung-Hak Cho is a Professor of Nanomechatronics from the University of Science and Technology in Republic of Korea. Also, he is a senior research scientist in KIMM(The Korea Institute of Machinery and Materials). He received M.E. and Ph. D degrees in electronics from Keio University Japan in 1997 and 2000, respectively. His current interests are development of advanced laser microprocessing techniques performing surface, 3-D microstructuring of transparent materials for applications, and Micro-LED display repair technology. He received several awards for his research and inventions in the area of laser microprocessing.